

THE SCATTERING PHASE: SEEN AT LAST

JEFFREY GALKOWSKI, PIERRE MARCHAND, JIAN WANG, AND MACIEJ ZWORSKI

ABSTRACT. The scattering phase, defined as $\log \det S(\lambda)/2\pi i$ where $S(\lambda)$ is the (unitary) scattering matrix, is the analogue of the counting function for eigenvalues when dealing with exterior domains and is closely related to Kreĭn’s spectral shift function. We revisit classical results on asymptotics of the scattering phase and point out that it is never monotone in the case of strong trapping of waves. Perhaps more importantly, we provide the first numerical calculations of scattering phases for non-radial scatterers. They show that the asymptotic Weyl law is accurate even at low frequencies and reveal effects of trapping such as lack of monotonicity. This is achieved by using the recent high level multiphysics finite element software **FreeFEM**.

1. INTRODUCTION

The scattering phase and its close relative, the spectral shift function, have been studied by mathematicians at least since the work of Birman and Kreĭn [BK62]. In the case of radial scattering, the scattering phase is the sum of phase shifts which are a central and classical topic in quantum scattering – see for instance [Sa20, §6.4].

The scattering phase is defined using the scattering matrix, $S(\lambda)$, which is a unitary operator mapping incoming waves to outgoing waves – see §2 and Figure 3. Because of its structure, the determinant of $S(\lambda)$ is well defined and we put

$$\sigma(\lambda) := \frac{1}{2\pi i} \log \det S(\lambda) \in \mathbb{R}, \quad \sigma(0) = 0, \quad (1.1)$$

where the last condition fixes the choice of log.

The scattering phase, $\sigma(\lambda)$, is appealing to mathematicians since it is a replacement for the counting function of eigenvalues for scattering problems – see [DyZw19a, §2.6, §3.9] and references given there. More precisely, as established by Jensen–Kato [JeKa78] and Bardos–Guillot–Ralston [BGR82], $\sigma(\lambda)$ satisfies

$$\mathrm{tr}(f(-\Delta_{\mathbb{R}^n \setminus \mathcal{O}}) - f(-\Delta)) = \int_0^\infty f(\lambda^2) \sigma'(\lambda) d\lambda, \quad f \in \mathcal{S}(\mathbb{R}). \quad (1.2)$$

Here, as in the rest of this paper, we specialized to the case of Dirichlet Laplacian, $\Delta_{\mathbb{R}^n \setminus \mathcal{O}}$ on $\mathbb{R}^n \setminus \mathcal{O}$, where $\mathcal{O} \Subset \mathbb{R}^n$ is an open set with a piecewise smooth boundary and connected complement. (Strictly speaking, $f(-\Delta_{\mathbb{R}^n \setminus \mathcal{O}})$ and $f(-\Delta)$ are defined on $L^2(\mathbb{R}^n \setminus \mathcal{O})$ and $L^2(\mathbb{R}^n)$, respectively, using the spectral theorem, but we consider the former space as subspace of $L^2(\mathbb{R}^n)$ using extension by 0.)

It could then be considered somewhat surprising that, to our knowledge, $\sigma(\lambda)$ has only been exhibited for radial scatterers. That is, there has never been any form of an actual assignment, via a numerical approximation, of $\lambda \mapsto \sigma(\lambda)$. At the time when asymptotic formulae for $\sigma(\lambda)$ were mathematically investigated (see §1.1) it is safe to say that such numerical computation were out of reach. Here we benefit from major advances in computational power and, in particular, from the recent high level multiphysics finite element software [FreeFEM](#) – see §4.

The numerical results for a variety of two dimensional scatterers \mathcal{O} are shown in our figures. The main conclusions are:

- The Weyl asymptotics for $\sigma(\lambda)$ given in (1.5) provide an accurate approximation starting at 0 energy; this accuracy is particularly striking in the case of non-trapping geometries – see Figure 1. They also appear remarkably accurate in trapping geometries.
- Strong trapping immediately causes lack of monotonicity of $\sigma(\lambda)$ which in accordance with (1.7) is related to the presence of resonances near the real axis (as reviewed in §1.2) – see top Figure 2.
- Mild trapping, illustrated in the two bottom Figures 2, does not seem to destroy monotonicity but there is a visible effect from scattering resonances at least for low frequencies.
- For star shaped obstacles the scattering phase is monotone [Ra78]. This monotonicity is not known for non-trapping obstacles even though [PePo82] provided full asymptotic expansion for $\sigma(\lambda)$; numerical examples suggest that $\sigma(\lambda)$ may always be monotone for non-trapping obstacles – see Figure 1. More experimentation would, however, be required for a firm conjecture.

1.1. **Weyl law for $\sigma(\lambda)$.** Possibly the most striking result about the counting function for the eigenvalues of the Dirichlet Laplacian, $\Delta_{\mathcal{O}}$, on a *bounded* domain $\mathcal{O} \subset \mathbb{R}^n$ is the Weyl law: with

$$N(\lambda) := |\text{Spec}(-\Delta_{\mathcal{O}}) \cap [0, \lambda^2]|,$$

$$N(\lambda) = \frac{\omega_n \text{vol}(\mathcal{O})}{(2\pi)^n} \lambda^n - \frac{\omega_{n-1} \text{vol}(\partial\mathcal{O})}{4(2\pi)^{n-1}} \lambda^{n-1} + o(\lambda^{n-1}), \quad (1.3)$$

where $\omega_n := \text{vol}(B_{\mathbb{R}^n}(0, 1))$. It was conjectured by Weyl in 1913 and established by Ivrii in 1980 (see [SaVa97] and [Iv16] for the history of this problem) under the assumptions that $\partial\mathcal{O}$ is smooth and the set of periodic orbits has measure zero (a generically valid fact expected to be true for all \mathcal{O} with smooth boundaries).

The trace formula (1.2) shows that $\sigma(\lambda)$ is the exact analogue of $N(\lambda)$ since $\text{tr } f(\Delta_{\mathcal{O}}) = \int_0^\infty f(\lambda^2) N'(\lambda) d\lambda$. It is then natural to ask if (1.3) holds for $\sigma(\lambda)$, with the understanding that, in agreement with (1.2) we now consider renormalized volume of $\mathbb{R}^n \setminus \mathcal{O}$. Hence

the natural analogue of (1.3) is given by

$$\sigma(\lambda) = -\frac{\omega_n \text{vol}(\mathcal{O})}{(2\pi)^n} \lambda^n - \frac{\omega_{n-1} \text{vol}(\partial\mathcal{O})}{4(2\pi)^{n-1}} \lambda^{n-1} + o(\lambda^{n-1}). \quad (1.4)$$

The difficulty in obtaining (1.4) stems from the fact that classical Tauberian theorems used for (1.3) use monotonicity of $N(\lambda)$. As we will see in §1.2, $\sigma(\lambda)$ is *not*, in general, monotone.

However, for star-shaped obstacles $\sigma'(\lambda) \leq 0$ was established by Helton–Ralston [Ra78] (see also [Ka78]). This monotonicity allowed Jensen–Kato [JeKa78] to obtain the leading term in (1.4) in that case (the convex case was treated by Buslaev [Bu75]). For convex obstacles Majda–Ralston [MaRa78–79] improved on [JeKa78] by obtaining a three term asymptotic expansion of $\sigma(\lambda)$. Using advances in propagation of singularities for obstacle problems (see [HöIII, Chapter 24] and references given there) Petkov–Popov [PePo82] obtained a *full* asymptotic expansion of $\sigma(\lambda)$ as $\lambda \rightarrow \infty$.

The first proof of (1.4) for all obstacles (for which the conditions after (1.3) hold) was given by Melrose [Me88] using his trace formula for scattering poles (see [DyZw19a, §3.10, §3.13]). Since that formula holds only in odd dimension the same restriction was imposed. This restriction was lifted using different methods by Robert [Ro94]. (A proof in all dimensions following Melrose’s idea can be given using [PeZw99].) In this historical account we only discussed the Dirichlet obstacle case. For more general perturbations see, for instance, [Ch98].

Specialized to two dimensions, (1.4) becomes

$$\sigma(\lambda) = -\frac{|\mathcal{O}|}{4\pi} \lambda^2 - \frac{|\partial\mathcal{O}|}{4\pi} \lambda + o(\lambda). \quad (1.5)$$

In the non-trapping case, in addition to further terms in (1.5), there is an asymptotic formula for $\sigma'(\lambda)$ [PePo82]. When a non-trapping \mathcal{O} has corners (i.e. has piecewise smooth, Lipschitz boundary) the following formula is suggested by heat expansions for interior problems which can be found in [Ch83, MaRo15]:

$$\sigma(\lambda) = -\frac{|\mathcal{O}|}{4\pi} \lambda^2 - \frac{|\partial\mathcal{O}|}{4\pi} \lambda + \frac{1}{24} \sum_j \left(\frac{\theta_j}{\pi} - \frac{\pi}{\theta_j} \right) - \frac{1}{24\pi} \int_{\partial\mathcal{O}} H ds + o(1), \quad (1.6)$$

where θ_j are the angles at the corners (measured from outside) and H is the curvature (with the convention that $H > 0$ for circles; we note that if there are no corners and connected \mathcal{O} , $\int_{\partial\mathcal{O}} H ds = 2\pi$). However, to our knowledge only the first asymptotic term of (1.6) is known rigorously in this case.

In the figures illustrating numerical results both asymptotic formulas are plotted against the computed scattering phase and its derivative. It is interesting to note that for most frequencies $\sigma'(\lambda)$ seems to agree with the asymptotic formula even in trapping

cases. This is similar to phenomena proved in the recent work of Lafontaine–Spence–Wunsch [LSW21] and perhaps could be rigorously established by similar methods.

1.2. Breit–Wigner approximation at high energies. Scattering resonances, which replace discrete spectral data for problems on unbounded domains, can be defined (in obstacle scattering) as poles of the meromorphic continuation of $S(\lambda)$ – see [DyZw19a, §4.4]. Since $S(\lambda)$, $\lambda > 0$ captures observable phenomena, it is interesting to see how those (complex) poles manifest themselves in its behaviour. The Breit–Wigner formula (see [DyZw19a, §2.2]) is one such way. In high energy obstacle scattering it was proved by Petkov–Zworski [PeZw99] and takes the following form:

$$\sigma'(\lambda) = \sum_{|\lambda_j - \lambda| < 1} \frac{1}{\pi} \frac{|\operatorname{Im} \lambda_j|}{|\lambda - \lambda_j|^2} + \mathcal{O}(\lambda^{n-1}), \quad (1.7)$$

where λ_j 's are the scattering resonances, that is the poles of $S(\lambda)$. From the point of view of the scattering asymptotics (1.4) we note that the sign of the Breit–Wigner terms (the sum of Lorentzians on the right in (1.7)) is opposite of the overall trend. In particular, if there exist λ_j 's with $|\operatorname{Im} \lambda_j| \ll (\operatorname{Re} \lambda_j)^{1-n}$, then $\sigma'(\lambda) > 0$ for λ near $\operatorname{Re} \lambda_j$. Strong trapping, such as that shown in Figure 2 (top figure), is known to produce resonances with $\operatorname{Im} \lambda_j = \mathcal{O}(|\lambda_j|^{-\infty})$ – see [St99], [TZ98]. Consequently, whenever such strong trapping occurs the scattering phase is *not* monotone.

The strong and parabolic trapping examples in Figures 2 (top two figures) show the presence of Lorentzians in σ' already at low energies. In the very weak trapping illustrated in the bottom Figure 2 there is some evidence of a low energy resonance but the effect seems minimal.

1.3. Low energy asymptotics. The numerical methods used to compute $\sigma'(\lambda)$ are not effective at very low energies – see §4. To obtain $\sigma(\lambda)$ by integration we used low energy asymptotic formulae for $\sigma'(\lambda)$. There has been recent progress on this subject and it is natural to review it here.

The first result we are aware of was obtained by Hassell–Zelditch [HaZe99] (using monotonicity of $\sigma(\lambda)$ as a function of the obstacle [Ra78]) and stated that $\sigma(\lambda) \sim \frac{1}{2} \log \lambda$. That was a by-product of their work on planar obstacles with the same scattering phase (an analogue of the isospectral problem). This result was successively improved by McGillivray [McG13], Strohmaier–Waters [StWa20] and Christiansen–Datchev [ChDa22] and a more precise asymptotic formula is given by

$$\sigma'(\lambda) \sim -\frac{2}{\lambda} \frac{1}{(-2 \log 2\lambda + C(\mathcal{O}) + 2\gamma)^2 + \pi^2} \quad (1.8)$$

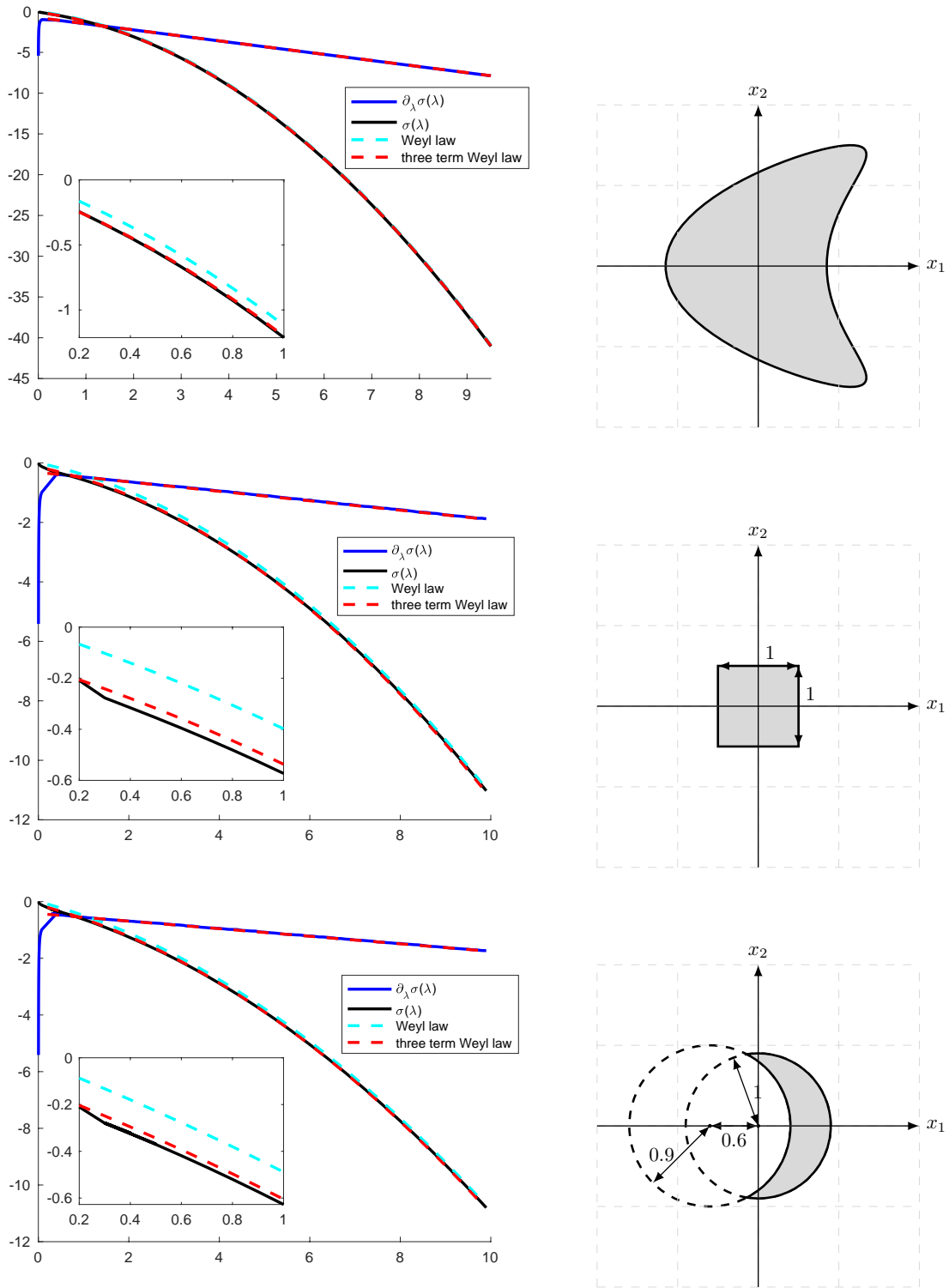


FIGURE 1. Scattering phase and the corresponding geometry: from top to bottom, a star-shaped obstacle, a star-shaped obstacle with corners, a non-trapping non-starshaped obstacle. We also indicate the comparisons with the Weyl law (1.5) and the (conjectural) three term Weyl for obstacles with corners (1.6).

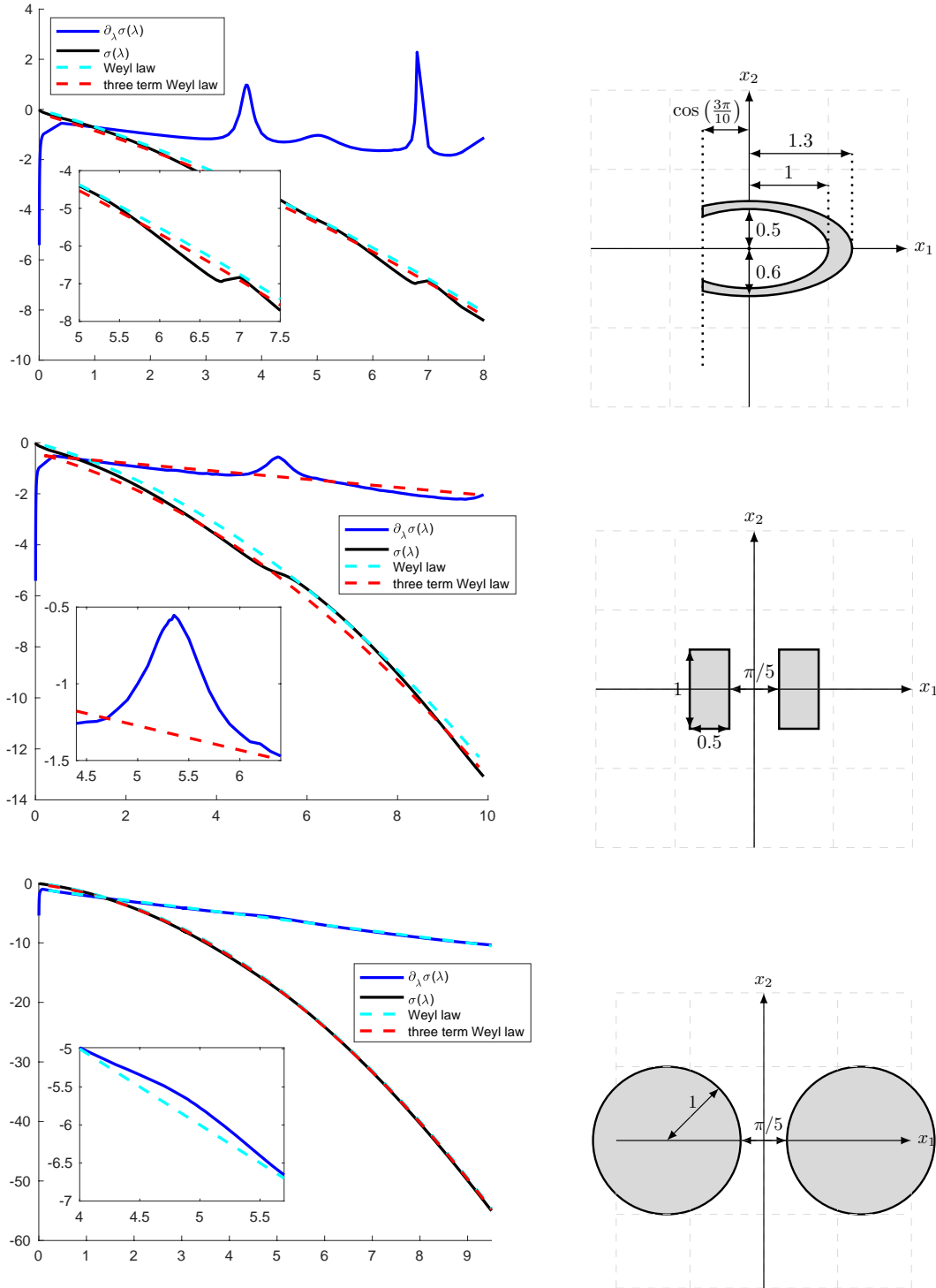


FIGURE 2. Scattering phase and the corresponding geometry: from top to bottom: strong trapping in a cavity, parabolic trapping from bouncing ball orbits, hyperbolic trapping in the form one closed orbit. In the case of strong trapping, we see numerical manifestations of (1.7). For the two rectangles, we expect resonances with $|\operatorname{Im} \lambda_j| \sim 1/|\lambda_j|$ so that (1.7) is inconclusive. In the case of two or more discs, the resonances satisfy $|\operatorname{Im} \lambda_j| > c$ (see [Va22] and references given there) and, as a result, at high energies their effect is weak.

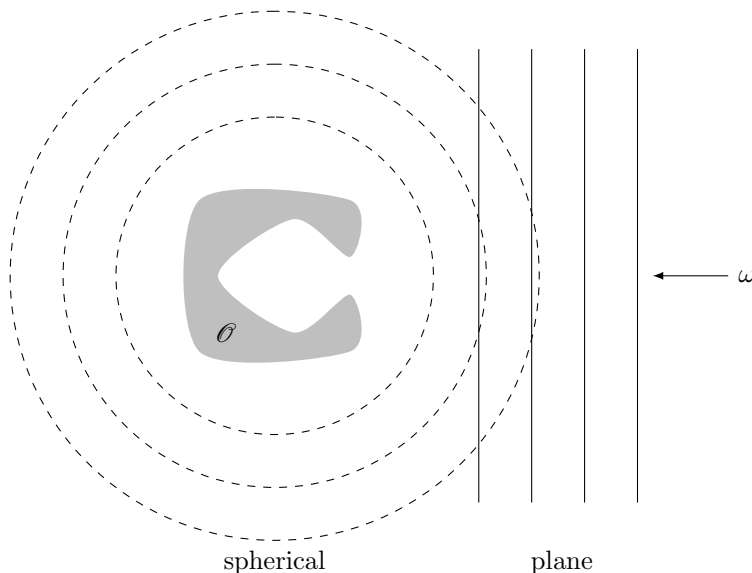


FIGURE 3. The waves used to define the scattering matrix

with $C(\mathcal{O})$ the logarithmic capacity of \mathcal{O} (see below) and γ the Euler constant. One way to define $C(\mathcal{O})$ is to consider the Green function of \mathcal{O} :

$$-\Delta G(x) = 0, \quad x \in \mathbb{R}^2 \setminus \mathcal{O}, \quad G(x) = 0, \quad x \in \partial\mathcal{O}, \quad G(x) \sim \log|x|, \quad |x| \rightarrow \infty,$$

Then

$$G(x) = \log|x| - C(\mathcal{O}) + o(1), \quad |x| \rightarrow \infty.$$

We only used the leading term to enhance the numerics.

Acknowledgements. The authors are grateful to Euan Spence for helpful conversations at the beginning of the project. JG was partially supported by EPSRC Early Career Fellowship EP/V001760/1 and Standard Grant EP/V051636/1, PM was partially supported by EPSRC grant EP/R005591/1, and MZ was partially supported by NSF grant DMS-1952939.

2. A FORMULA FOR THE DERIVATIVE OF THE SCATTERING PHASE

In order to compute $\sigma(\lambda)$ we recall a definition of the scattering matrix in dimension $n = 2$ – for motivation and a detailed presentation see [DyZw19a, §3.7, §4.4].

We start with perturbed plane waves – see (2.3) below. For that we let $\omega \in \mathbb{S}^1$, $\lambda \in \mathbb{R}$ and define $u(\lambda, \cdot, \omega) \in C^\infty(\mathbb{R}^2)$ as the unique *outgoing* solution to

$$(-\Delta - \lambda^2)u = 0 \quad \text{in } \mathbb{R}^2 \setminus \mathcal{O}, \quad u|_{\partial\mathcal{O}} = -e^{i\lambda\langle x, \omega \rangle}|_{\partial\mathcal{O}}. \quad (2.1)$$

(We note that, to streamline notation, the convention is slightly different than in [DyZw19a].) Here, by *outgoing*, we mean that there is $b(\lambda, \cdot, \omega) \in C^\infty(\mathbb{S}^1)$ such that

$$u(\lambda, x, \omega) = e^{-\frac{\pi i}{4}} \sqrt{2\pi/(\lambda|x|)} e^{i\lambda|x|} b(\lambda, x/|x|, \omega) + O(|x|^{-3/2}). \quad (2.2)$$

We then define

$$e(\lambda, x, \omega) := e^{i\lambda\langle x, \omega \rangle} + u(\lambda, x, \omega). \quad (2.3)$$

The scattering matrix, $S(\lambda) : L^2(\mathbb{S}^1) \rightarrow L^2(\mathbb{S}^1)$, is then given by $S(\lambda) := I + A(\lambda)$, where $A(\lambda)$ is an integral operator defined as

$$A(\lambda)f(\theta) := \int_{\mathbb{S}^1} A(\lambda, \theta, \omega) f(\omega) d\omega, \quad A(\lambda, \theta, \omega) := b(\lambda, \theta, \omega). \quad (2.4)$$

The scattering matrix $S(\lambda)$ is unitary and extends meromorphically to the Riemann surface of $\log \lambda$.

It will be useful when computing the scattering phase to rewrite the integral kernel $A(\lambda, \theta, \omega)$ as an integral over $\partial\mathcal{O}$:

Lemma 1. *Let ν denote unit normal to $\partial\mathcal{O}$ pointing out of \mathcal{O} . Then, in the notation of (2.3), we have (with $ds(x)$ the line measure on $\partial\mathcal{O}$ or $\partial B(0, r)$)*

$$A(\lambda, \theta, \omega) = \frac{1}{4\pi i} \int_{\partial\mathcal{O}} e^{-i\lambda\langle x, \theta \rangle} \partial_\nu e(\lambda, x, \omega) ds(x). \quad (2.5)$$

Proof. Green's formula shows that, with $e(x) := e(\lambda, x, \omega)$ and $\mathcal{O} \subset B(0, R)$

$$\begin{aligned} 0 &= \int_{B(0, R) \setminus \mathcal{O}} ([(-\Delta - \lambda^2)e(x)](e^{-i\lambda\langle x, \theta \rangle}) - e(x)[(-\Delta - \lambda^2)e^{-i\lambda\langle x, \theta \rangle}]) dx \\ &= \int_{\partial\mathcal{O}} e^{-i\lambda\langle x, \theta \rangle} \partial_\nu e(x) ds(x) - \int_{\partial B(0, R)} (\partial_r e(x) e^{-i\lambda\langle x, \theta \rangle} - e(x) \partial_r [e^{-i\lambda\langle x, \theta \rangle}]) ds(x). \end{aligned} \quad (2.6)$$

To compute the last term in (2.6), we use the formulae (2.2) and (2.3) together with the stationary phase method (see [DyZw19a, Theorem 3.38]): for $a \in C^\infty(\mathbb{S}^1)$,

$$\int_{\partial B(0, R)} a(x/|x|) e^{-i\lambda\langle x, \theta \rangle} ds(x) = \sqrt{2\pi R/\lambda} (e^{-\frac{i\pi}{4}} a(-\theta) e^{i\lambda R} + e^{\frac{i\pi}{4}} a(\theta) e^{-i\lambda R}) + \mathcal{O}(R^{-\frac{1}{2}}). \quad (2.7)$$

By applying (2.7) when $\theta \neq \omega$, and the $x \mapsto -x$ symmetry when $\omega = \theta$, we obtain $\int_{\partial B(0, R)} \langle x/|x|, \omega + \theta \rangle e^{i\lambda\langle x, \omega - \theta \rangle} ds(x) = \mathcal{O}(R^{-\frac{1}{2}})$. This and (2.3) give, with $u(x) := u(\lambda, x, \omega)$,

$$\begin{aligned} &\int_{\partial B(0, R)} (\partial_r e(x) e^{-i\lambda\langle x, \theta \rangle} - e(x) \partial_r [e^{-i\lambda\langle x, \theta \rangle}]) ds(x) = \\ &\int_{\partial B(0, R)} (\partial_r u(x) + i\lambda \langle x/|x|, \theta \rangle u(x)) e^{-i\lambda\langle x, \theta \rangle} ds(x) + \mathcal{O}(R^{-\frac{1}{2}}). \end{aligned}$$

In the notation of (2.2), we put $B := e^{-\pi i/4} \sqrt{2\pi/\lambda} b(\lambda, x/|x|, \omega)$ and then apply (2.7) to see that this expression is equal to

$$e^{i\lambda R} R^{-\frac{1}{2}} \int_{\partial B(0,R)} (i\lambda + i\lambda \langle x/|x|, \theta \rangle) B e^{-i\lambda \langle x, \theta \rangle} ds(x) + \mathcal{O}(R^{-\frac{1}{2}}) = 4\pi i b(\lambda, \theta, \omega) + \mathcal{O}(R^{-\frac{1}{2}}).$$

Combined with (2.6) and (2.4) this completes the proof of (2.5) by taking $R \rightarrow \infty$. \square

Remarks. 1. For evaluating the traces in Lemma 2 numerically we note that, using a positive parametrization $[0, L) \rightarrow \partial \mathcal{O}$, $s \mapsto x = x(s)$, $|\dot{x}| = 1$, $\nu(s) = (\dot{x}_2(s), -\dot{x}_1(s))$ (ν is the outward normal),

$$\begin{aligned} \partial_\nu(e^{i\lambda \langle x, \omega \rangle}) &= i\lambda \langle \dot{x}, \omega^\perp \rangle e^{i\lambda \langle x, \omega \rangle}, \\ \mathbb{S}^1 \ni \omega &= (\cos t, \sin t), \quad \omega^\perp := (-\sin t, \cos t), \quad t \in [0, 2\pi). \end{aligned} \tag{2.8}$$

2. We recall the following symmetry of $e(\lambda, x, \omega)$ [DyZw19a, Theorem 4.20]:

$$\overline{e(\lambda, x, \omega)} = e(-\lambda, x, \omega).$$

Next, we calculate a formula for $\sigma'(\lambda)$ in terms of $e(\lambda, x, \omega)$. The definitions give

$$\sigma'(\lambda) = \frac{1}{2\pi i} \operatorname{tr} S(\lambda)^* \partial_\lambda S(\lambda) = \frac{1}{2\pi i} \operatorname{tr} \partial_\lambda A(\lambda) + \frac{1}{2\pi i} \operatorname{tr} A(\lambda)^* \partial_\lambda A(\lambda). \tag{2.9}$$

We start with the first term on the right hand side of (2.9):

Lemma 2. *We have*

$$\operatorname{tr} \partial_\lambda A(\lambda) = \frac{1}{4\pi} \int_{\mathbb{S}^1} \int_{\partial \mathcal{O}} e^{-i\lambda \langle x, \omega \rangle} G(\lambda, x, \omega) ds(x) d\omega, \tag{2.10}$$

where, in the notation of (2.3),

$$\begin{aligned} G(\lambda, x, \omega) &:= -\langle x, \omega \rangle \partial_\nu u(\lambda, x, \omega) + \partial_\nu v(\lambda, x, \omega), \\ (-\Delta - \lambda^2)v(\lambda, x, \omega) &= -2i\lambda u(\lambda, x, \omega), \quad x \in \mathbb{R}^2 \setminus \mathcal{O}, \\ v(\lambda, x, \omega)|_{\partial \mathcal{O}} &= -\langle x, \omega \rangle e^{i\lambda \langle x, \omega \rangle}|_{\partial \mathcal{O}}. \end{aligned} \tag{2.11}$$

Proof. The integral kernel of $\partial_\lambda A(\lambda)$ is given by

$$\partial_\lambda A(\lambda, \theta, \omega) = \frac{1}{4\pi i} \int_{\partial \mathcal{O}} (\partial_\lambda [e^{-i\lambda \langle x, \theta \rangle}] \partial_\nu e(\lambda, x, \omega) + e^{-i\lambda \langle x, \theta \rangle} \partial_\nu \partial_\lambda e(\lambda, x, \omega)) ds(x). \tag{2.12}$$

From (2.3) we see that $\partial_\lambda e(\lambda, x, \omega) = i\langle x, \omega \rangle e^{i\lambda \langle x, \omega \rangle} + iv(\lambda, x, \omega)$, where v is defined in the statement of the lemma. Hence, in the notation of (2.8), and with $e := e(\lambda, x, \omega)$, the integrand in (2.12) for $\theta = \omega$ is given by

$$i\langle \dot{x}, \omega^\perp \rangle + i(-\langle x, \omega \rangle \partial_\nu u(\lambda, x, \omega) + \partial_\nu v(\lambda, x, \omega)) e^{-i\lambda \langle x, \omega \rangle}.$$

This gives (2.10) since $\int_{\partial \mathcal{O}} \langle \dot{x}, \omega^\perp \rangle ds = 0$. \square

We now move to the second term in (2.9):

Lemma 3. *We have*

$$\operatorname{tr} A(\lambda)^* \partial_\lambda A(\lambda) = \frac{1}{16\pi^2} \int_{\mathbb{S}^1} \int_{\mathbb{S}^1} H(\lambda, \omega, \theta) F(\lambda, \omega, \theta) d\omega d\theta, \quad (2.13)$$

where in the notation of Lemma 2,

$$H := \int_{\partial\mathcal{O}} e^{i\lambda\langle x, \theta \rangle} \left(-i\lambda\langle \dot{x}, \omega^\perp \rangle e^{-i\lambda\langle x, \omega \rangle} + \overline{\partial_\nu u(\lambda, x, \omega)} \right) ds(x),$$

$$F := \int_{\partial\mathcal{O}} e^{-i\lambda\langle y, \theta \rangle} \left[(\langle \dot{y}, \omega^\perp \rangle)(\lambda\langle y, \theta - \omega \rangle + i)e^{i\lambda\langle y, \omega \rangle} - i\langle y, \theta \rangle \partial_\nu u(\lambda, y, \omega) + i\partial_\nu v(\lambda, y, \omega) \right] ds(y).$$

Proof. The integral kernel of $A(\lambda)^*$ is given by

$$A^*(\lambda, \omega, \theta) = -\frac{1}{4\pi i} \int_{\partial\mathcal{O}} e^{i\lambda\langle x, \theta \rangle} \overline{\partial_\nu e(\lambda, x, \omega)} ds(x),$$

and hence $\operatorname{tr} A(\lambda)^* \partial_\lambda A(\lambda)$ is given as an integral over $\partial\mathcal{O}_x \times \partial\mathcal{O}_y \times \mathbb{S}_\theta^1 \times \mathbb{S}_\omega^1$ of

$$\frac{1}{16\pi^2} e^{i\lambda\langle x-y, \theta \rangle} \overline{\partial_\nu e(\lambda, x, \omega)} (-i\langle y, \theta \rangle \partial_\nu e(\lambda, y, \omega) + \partial_\nu \partial_\lambda e(\lambda, y, \omega)).$$

Using $\partial_\lambda e(\lambda, x, \omega) = i\langle x, \omega \rangle e^{i\lambda\langle x, \omega \rangle} + iv(\lambda, x, \omega)$ and the definition of $e(\lambda, x, \omega)$ completes the proof. \square

Remark. The integral over θ could be eliminated using Bessel functions. That however introduces factors $J_0(\lambda|x-y|)$ and $\langle y, x-y \rangle J_1(\lambda|x-y|)/|x-y|$ and destroys the product structure which only requires separate integration in x and y . Hence, it is not numerically advantageous.

3. ANALYTIC SOLUTION FOR THE DISC

In order to validate our numerical scheme, the scheme was tested against the analytic solution for \mathcal{O} given by the unit disk. We record in this section the formulae for both $\sigma(\lambda)$ and $u(\lambda, x, \omega)$ in this case.

3.1. The scattering phase for the unit disk. To compute the scattering phase for the disk, we use polar coordinates and separation of variables to find the scattering matrix. In particular, in polar coordinates (r, θ) , a solution to $(-\Delta - \lambda^2)u = 0$ with $u|_{\partial B(0,1)}$ with $u(r, \theta) = \sum_n e^{in\theta} u_n(r)$ satisfies

$$\left(-\partial_r^2 - \frac{1}{r} \partial_r u + \frac{n^2}{r^2} - \lambda^2 \right) u_n(r) = 0, \quad u_n(1) = 0$$

and hence

$$u_n(r) = A_n \left(-\frac{H_{|n|}^{(2)}(\lambda)}{H_{|n|}^{(1)}(\lambda)} H_{|n|}^{(1)}(\lambda r) + H_{|n|}^{(2)}(\lambda r) \right). \quad (3.1)$$

Recall [DLMF, §10.17(i)] that for $\lambda, r > 0$, $n \geq 0$, we have

$$\begin{aligned} H_n^{(1)}(\lambda r) &= \left(\frac{2}{\pi \lambda r}\right)^{1/2} e^{i(\lambda r - \frac{1}{2}n\pi - \frac{1}{4}\pi)} + O(r^{-3/2}), \\ H_n^{(2)}(\lambda r) &= \left(\frac{2}{\pi \lambda r}\right)^{1/2} e^{-i(\lambda r - \frac{1}{2}n\pi - \frac{1}{4}\pi)} + O(r^{-3/2}). \end{aligned}$$

Thus, $H_{|n|}^{(1)}(\lambda r)$ is outgoing and $H_{|n|}^{(2)}(\lambda r)$ is incoming and hence this implies that $\sin(n\theta)$ ($n \neq 0$) and $\cos(n\theta)$ are eigenfunctions of $S(\lambda)$ with eigenvalue

$$\mu_n := (-1)^{n+1} \frac{H_{|n|}^{(2)}(\lambda)}{H_{|n|}^{(1)}(\lambda)}.$$

In particular, using the Wronskian relation [DLMF, (10.5.5)] in the last line, we obtain

$$\begin{aligned} \sigma'(\lambda) &= \left(\frac{1}{2\pi i} \log \det S(\lambda)\right)' \\ &= \frac{R}{2\pi i} \sum_{n=-\infty}^{\infty} \frac{(H_{|n|}^{(2)})'(\lambda)}{H_{|n|}^{(2)}(\lambda)} - \frac{(H_{|n|}^{(1)})'(\lambda)}{H_{|n|}^{(1)}(\lambda)} \\ &= -\frac{2}{\pi^2 \lambda} \sum_{n=-\infty}^{\infty} \frac{1}{H_{|n|}^{(1)}(\lambda) H_{|n|}^{(2)}(\lambda)}. \end{aligned} \tag{3.2}$$

Remark. Note that we do not write $\sigma(\lambda)$ directly since this would involve making a choice of branch for the logarithm. We instead use the $\sigma(0) = 0$ to make this choice when integrating $\sigma'(\lambda)$.

3.2. The scattering amplitude for the unit disk. The incoming portion of $e(\lambda)$ in (2.3) is given by the incoming portion of $e^{i\lambda\langle x, \omega \rangle}$. Using the Jacobi–Anger expansion, with $x = r(\cos \theta, \sin \theta)$ we have

$$\begin{aligned} e^{i\lambda\langle x, \omega \rangle} &= e^{i\lambda r(\cos \theta \cos \omega + \sin \theta \sin \omega)} = e^{i\lambda r \cos(\theta - \omega)} \\ &= \sum_{n=0}^{\infty} \delta_n i^n (H_n^{(1)}(\lambda r) + H_n^{(2)}(\lambda r)) \cos(n(\theta - \omega)), \end{aligned}$$

where $\delta_0 = \frac{1}{2}$ and $\delta_n = 1$ for $n > 0$. Thus, from (3.1) we have

$$e(\lambda, r\theta, \omega) = \sum_{n=0}^{\infty} \delta_n i^n \left(-\frac{H_n^{(2)}(\lambda)}{H_n^{(1)}(\lambda)} H_n^{(1)}(\lambda r) + H_n^{(2)}(\lambda r) \right) \cos(n(\theta - \omega)),$$

and hence

$$u(\lambda, r\theta, \omega) = \sum_{n=0}^{\infty} \delta_n i^n \left(1 - \frac{H_n^{(2)}(\lambda)}{H_n^{(1)}(\lambda)} \right) H_n^{(1)}(\lambda r) \cos(n(\theta - \omega)). \tag{3.3}$$

We can now easily deduce explicit expression for v , $\partial_\nu u$ and $\partial_\nu v$.

4. NUMERICAL SCHEME

In this section we describe the numerical scheme used to compute the scattering phase.

4.1. Setup. To compute (2.10) and (2.13), we use the trapezoidal rule to approximate the 1-d integrals along the angles θ and ω : for $N > 0$, $\omega_l = 2\pi l/N$ for $l = 0 \cdots N-1$, and using the 2π -periodicity, we use the following approximations

$$\mathrm{tr} \partial_\lambda A \approx \frac{1}{4\pi} \frac{2\pi}{N} \sum_{l=0}^{N-1} \int_{\partial\mathcal{O}} e^{-\lambda\langle\omega_l, x\rangle} G(\lambda, x, \omega_l) ds(x),$$

where G is given in (2.11). For the second term we benefit from the factorization in which we only compute two integrals over the boundary:

$$\mathrm{tr} A^* \partial_\lambda A \approx \frac{1}{16\pi^2} \left(\frac{2\pi}{N}\right)^2 \sum_{l=0}^{N-1} \sum_{p=0}^{N-1} H(\lambda, \omega_l, \theta_p) F(\lambda, \omega_l, \theta_p),$$

where H and F are given in Lemma 3. It remains compute the normal derivatives of $u(\lambda, \cdot, \omega)$ and $v(\lambda, \cdot, \omega)$ for $\omega \in (\omega_l)_{l=0}^{N-1}$.

To approximate u and v , we first need to reformulate both problems on a bounded domain in $\mathbb{R}^2 \setminus \overline{\mathcal{O}}$. We use the method of *Perfectly Matched Layers* (PML) (introduced in [Be1994] for electromagnetic waves) to do this. More precisely, we use a radial PML [CoMo98]: consider a disk $B_{R_{\mathrm{PML}}}$ with $R_{\mathrm{PML}} > R_{\mathrm{DOM}}$ such that $\overline{\mathcal{O}} \subsetneq B_{R_{\mathrm{DOM}}}$, we reformulate both (2.1) and (2.11) using polar coordinates (r, θ) in $B_{R_{\mathrm{PML}}}$, and we apply a complex scaling $\hat{r} = r + \frac{i}{\lambda} \int_0^r \gamma(s) ds$ where γ is an increasing function defined on $[0, R_{\mathrm{PML}})$ and equal to zero in $[0, R_{\mathrm{DOM}})$. Several choices can be made for γ , we choose $\gamma(r) := 1/(R_{\mathrm{PML}} - r)$ for $r \in [R_{\mathrm{DOM}}, R_{\mathrm{PML}})$ as advocated in [Ber*98]. We denote $\mathbf{J}_{\mathrm{PML}}$ the Jacobian of the transformation from the Cartesian coordinates to the complexified Cartesian coordinates.

The equations for u and v , (2.1) and (2.11) are solved with the Galerkin method using Lagrange finite elements; i.e. we solve these equations in a finite-dimensional subspace $V_h \subset H^1(B_{R_{\mathrm{PML}}} \setminus \overline{\mathcal{O}})$ formed by piecewise-polynomial functions on a mesh, and we denote h the mesh element size (see [ErGu22] for more information): we find $u_h, v_h \in V_h$ such that $u_h|_{\partial\mathcal{O}} = -\mathcal{I}_h(e^{i\lambda\langle x, \omega \rangle})|_{\partial\mathcal{O}}$, $v_h|_{\partial\mathcal{O}} = -\mathcal{I}_h(\lambda\langle x, \omega \rangle e^{i\lambda\langle x, \omega \rangle})|_{\partial\mathcal{O}}$ where $\mathcal{I}_h : C^0(\overline{B_{R_{\mathrm{PML}}} \setminus \overline{\mathcal{O}}}) \rightarrow V_h$ is the Lagrange interpolation operator, $u_h|_{\partial B_{\mathrm{PML}}} = v_h|_{\partial B_{\mathrm{PML}}} = 0$,

$$a(u_h, w_h) = 0 \text{ for all } w_h \in V_{h,0}, \text{ and } a(v_h, w_h) = b_{u_h}(w_h) \text{ for all } w_h \in V_{h,0},$$

where $V_{h,0}$ is the subspace of functions in V_h whose value on $\partial\mathcal{O} \cup \partial B_{\text{PML}}$ is zero,

$$\begin{aligned} a(u, w) &= \int_{B_{R_{\text{DOM}}}\setminus\bar{\mathcal{O}}} (\nabla u \cdot \nabla w - \lambda^2 u w) dx dy \\ &\quad + \int_{B_{R_{\text{PML}}}\setminus\bar{B}_{R_{\text{DOM}}}} (\mathbf{J}_{\text{PML}}^{-T} \nabla u \cdot \mathbf{J}_{\text{PML}}^{-T} \nabla w - \lambda^2 u w) |\det \mathbf{J}_{\text{PML}}| dx dy, \\ b_{u_h}(w) &= -2i\lambda \int_{B_{R_{\text{PML}}}} u_h w |\det \mathbf{J}_{\text{PML}}| dx dy. \end{aligned}$$

In our numerical experiments, the approximation space V_h is spanned by \mathbb{P}_2 Lagrange elements, i.e. continuous piecewise quadratic functions. To bound the error from discretization independently of λ when solving (2.1) and (2.11), we need $h^{2p}\lambda^{2p+1} = h^4\lambda^5$ bounded [DuWu15], where h is the mesh size and p is the degree of the finite element functions. To satisfy this condition, we set the number of points per wavelength to $\mu \times (1 + \lambda^{1/4})$, where μ is a constant. Differentiating u_h and v_h to take the Neumann trace on $\partial\mathcal{O}$, we obtain \mathbb{P}_1 Lagrange elements on the discretization of $\partial\mathcal{O}$, which can then be used to compute $G(\lambda, x, \omega_l)$, $H(\lambda, \omega_l, \theta_p)$ and $F(\lambda, \omega_l, \theta_p)$.

Note that these approximations depend on λ and the angle w_l in the Dirichlet conditions, and thus require solving (2.1) and (2.11) for N different angles and hence N different right-hand sides, for a given frequency λ . Thus, for a given λ , we factorize the matrix stemming from the discretization (note that it is the same for both u_h and v_h), and we use it to solve the discretized problems with several right-hand sides at the same time to improve efficiency. The numerical computations were carried out with FreeFEM [He12]. More precisely, we used its interface with PETSc [Ba*19] to solve linear systems with MUMPS [Am*01, Am*06].

Remark. Since we only need the Neumann traces of u and v to compute the scattering phase, it is quite natural to want to reformulate both problems (2.1) and (2.11) using Boundary Integral Equations (BIE). While (2.1) can easily be reformulated with a standard BIE, the presence of a right-hand side in (2.11) makes it less convenient to usual boundary integral formulations. Nevertheless, it should be possible to represent v differentiating Green's third identity (which we can use to represent u), but it would imply non-standard boundary integral operators. Thus, we preferred to use more standard tools such as PML.

4.2. Convergence. When \mathcal{O} is a disk, we use the analytical expression from (3.2), with a truncated sum using $|n| \leq 5\lambda$, to compute the relative error on σ' . In Table 1, from left to right, the frequency λ is increasing. The tables at the top have $R_{\text{PML}} - R_{\text{DOM}} = 0.25$, while tables at the bottom keep a number of mesh cells in the PML region constant, $R_{\text{PML}} - R_{\text{DOM}} = 5h$.

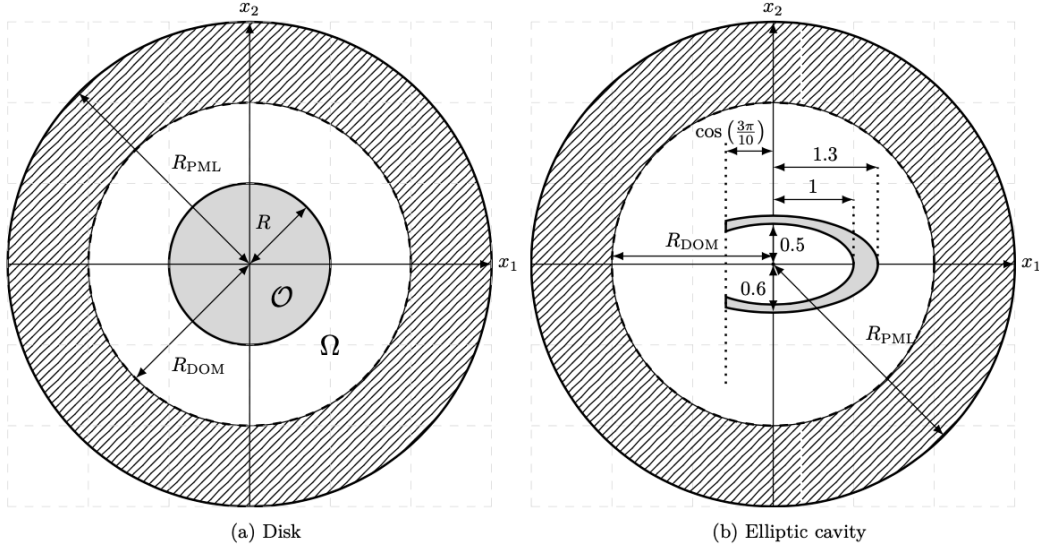


FIGURE 4. Considered geometries with their PML

For a fixed $R_{\text{PML}} - R_{\text{DOM}}$ and λ increasing (tables at the top in Table 1), the error is decreasing, which is consistent with [GLS21], which states that the error on u should decrease in this case. We also observed that keeping a fixed number of mesh cells in the PML region (tables at the bottom in Table 1) is enough to have the same level of precision as with a fixed PML region. This is due to the particular choice of γ , and we do not observe this behaviour with other usual complex scaling (taking γ as a linear or quadratic function for example). The advantage is that, in this case, $R_{\text{PML}} - R_{\text{DOM}}$ decreases so that the computational cost is reduced compared to keeping $R_{\text{PML}} - R_{\text{DOM}}$ constant.

Table 2 gives the relative error on σ' with N increasing, $\mu = 20$, $R_{\text{DOM}} = 2$ and $R_{\text{PML}} - R_{\text{DOM}} = 5h$. We observe that we need to take N large enough to converge to the same level of error as in Table 1, and N needs to be larger for larger λ : $N = 30$ for $\lambda = 10$ and $N = 50$ for $\lambda = 10$. This is consistent with the fact that u and v are more and more oscillatory when λ increases, and we observed numerically that taking $N \sim \lambda$ is sufficient to keep the error bounded independently of λ .

4.3. Main numerical results. The values of σ' in Figure 1 are obtained for $\lambda \geq 3$ with $\mu = 30$, $R_{\text{PML}} - R_{\text{DOM}} = 5h$ and $N = 10\lambda$. For $0.3 \leq \lambda < 3$, we computed σ' , but this required the use of significantly larger μ : usually $\mu = 300$ for $0.3 \leq \lambda \leq 2$ and $\mu = 200$ for $2 \leq \lambda \leq 3$. Figure 2 was produced in the same way, except that we took $\mu = 100$ away from an interval of size 0.2 centered on the quasimode frequencies (which are explicitly computable using the eigenvalues of the Laplacian in the ellipse, see [MGSS22, Section 1.1.3]). On the intervals near quasimode frequencies we also

<table border="1" style="width: 100%; border-collapse: collapse;"> <thead> <tr> <th style="text-align: left;">μ</th> <th style="text-align: left;">Relative error on σ'</th> </tr> </thead> <tbody> <tr><td>1</td><td>0.1519</td></tr> <tr><td>5</td><td>0.0120</td></tr> <tr><td>10</td><td>0.0038</td></tr> <tr><td>15</td><td>0.0023</td></tr> <tr><td>20</td><td>0.0015</td></tr> </tbody> </table>	μ	Relative error on σ'	1	0.1519	5	0.0120	10	0.0038	15	0.0023	20	0.0015	<table border="1" style="width: 100%; border-collapse: collapse;"> <thead> <tr> <th style="text-align: left;">μ</th> <th style="text-align: left;">Relative error on σ'</th> </tr> </thead> <tbody> <tr><td>1</td><td>0.0258</td></tr> <tr><td>5</td><td>0.0097</td></tr> <tr><td>10</td><td>0.0030</td></tr> <tr><td>15</td><td>0.0016</td></tr> <tr><td>20</td><td>0.0008</td></tr> </tbody> </table>	μ	Relative error on σ'	1	0.0258	5	0.0097	10	0.0030	15	0.0016	20	0.0008
μ	Relative error on σ'																								
1	0.1519																								
5	0.0120																								
10	0.0038																								
15	0.0023																								
20	0.0015																								
μ	Relative error on σ'																								
1	0.0258																								
5	0.0097																								
10	0.0030																								
15	0.0016																								
20	0.0008																								
$\lambda = 10, R_{\text{PML}} - R_{\text{DOM}} = 0.25$	$\lambda = 20, R_{\text{PML}} - R_{\text{DOM}} = 0.25$																								
<table border="1" style="width: 100%; border-collapse: collapse;"> <thead> <tr> <th style="text-align: left;">μ</th> <th style="text-align: left;">Relative error on σ'</th> </tr> </thead> <tbody> <tr><td>1</td><td>0.0779</td></tr> <tr><td>5</td><td>0.0108</td></tr> <tr><td>10</td><td>0.0038</td></tr> <tr><td>15</td><td>0.0021</td></tr> <tr><td>20</td><td>0.0015</td></tr> </tbody> </table>	μ	Relative error on σ'	1	0.0779	5	0.0108	10	0.0038	15	0.0021	20	0.0015	<table border="1" style="width: 100%; border-collapse: collapse;"> <thead> <tr> <th style="text-align: left;">μ</th> <th style="text-align: left;">Relative error on σ'</th> </tr> </thead> <tbody> <tr><td>1</td><td>0.0334</td></tr> <tr><td>5</td><td>0.0096</td></tr> <tr><td>10</td><td>0.0030</td></tr> <tr><td>15</td><td>0.0015</td></tr> <tr><td>20</td><td>0.0008</td></tr> </tbody> </table>	μ	Relative error on σ'	1	0.0334	5	0.0096	10	0.0030	15	0.0015	20	0.0008
μ	Relative error on σ'																								
1	0.0779																								
5	0.0108																								
10	0.0038																								
15	0.0021																								
20	0.0015																								
μ	Relative error on σ'																								
1	0.0334																								
5	0.0096																								
10	0.0030																								
15	0.0015																								
20	0.0008																								
$\lambda = 10, R_{\text{PML}} - R_{\text{DOM}} = 5h$	$\lambda = 20, R_{\text{PML}} - R_{\text{DOM}} = 5h$																								

TABLE 1. Relative error on σ' for a disk with $R_{\text{DOM}} = 2$ and $N = 100$.

<table border="1" style="width: 100%; border-collapse: collapse;"> <thead> <tr> <th style="text-align: left;">μ</th> <th style="text-align: left;">N</th> <th style="text-align: left;">Relative error on σ'</th> </tr> </thead> <tbody> <tr><td>20</td><td>20</td><td>0.0594</td></tr> <tr><td>20</td><td>25</td><td>0.0025</td></tr> <tr><td>20</td><td>30</td><td>0.0015</td></tr> <tr><td>20</td><td>35</td><td>0.0015</td></tr> <tr><td>20</td><td>40</td><td>0.0015</td></tr> <tr><td>20</td><td>45</td><td>0.0015</td></tr> <tr><td>20</td><td>50</td><td>0.0015</td></tr> <tr><td>20</td><td>55</td><td>0.0015</td></tr> <tr><td>20</td><td>60</td><td>0.0015</td></tr> </tbody> </table>	μ	N	Relative error on σ'	20	20	0.0594	20	25	0.0025	20	30	0.0015	20	35	0.0015	20	40	0.0015	20	45	0.0015	20	50	0.0015	20	55	0.0015	20	60	0.0015	<table border="1" style="width: 100%; border-collapse: collapse;"> <thead> <tr> <th style="text-align: left;">μ</th> <th style="text-align: left;">N</th> <th style="text-align: left;">Relative error on σ'</th> </tr> </thead> <tbody> <tr><td>20</td><td>20</td><td>0.0618</td></tr> <tr><td>20</td><td>25</td><td>0.0310</td></tr> <tr><td>20</td><td>30</td><td>0.0309</td></tr> <tr><td>20</td><td>35</td><td>0.0311</td></tr> <tr><td>20</td><td>40</td><td>0.0307</td></tr> <tr><td>20</td><td>45</td><td>0.0031</td></tr> <tr><td>20</td><td>50</td><td>0.0008</td></tr> <tr><td>20</td><td>55</td><td>0.0008</td></tr> <tr><td>20</td><td>60</td><td>0.0008</td></tr> </tbody> </table>	μ	N	Relative error on σ'	20	20	0.0618	20	25	0.0310	20	30	0.0309	20	35	0.0311	20	40	0.0307	20	45	0.0031	20	50	0.0008	20	55	0.0008	20	60	0.0008
μ	N	Relative error on σ'																																																											
20	20	0.0594																																																											
20	25	0.0025																																																											
20	30	0.0015																																																											
20	35	0.0015																																																											
20	40	0.0015																																																											
20	45	0.0015																																																											
20	50	0.0015																																																											
20	55	0.0015																																																											
20	60	0.0015																																																											
μ	N	Relative error on σ'																																																											
20	20	0.0618																																																											
20	25	0.0310																																																											
20	30	0.0309																																																											
20	35	0.0311																																																											
20	40	0.0307																																																											
20	45	0.0031																																																											
20	50	0.0008																																																											
20	55	0.0008																																																											
20	60	0.0008																																																											
$\lambda = 10$	$\lambda = 20$																																																												

TABLE 2. Relative error on σ' for a disk with $R_{\text{DOM}} = 2$ and $R_{\text{PML}} - R_{\text{DOM}} = 5h$

needed to increase μ significantly, and we took $\mu = 300$. For every geometry, we refined the mesh around corners in order to obtain good precision.

REFERENCES

- [Am*01] P.R. Amestoy I.S. Duff, J.-Y. L'Excellent and J. Koster, *A Fully Asynchronous Multifrontal Solver Using Distributed Dynamic Scheduling*, SIAM Journal on Matrix Analysis and Applications, **23**(2001), 15–41.

- [Am*06] P.R. Amestoy, A. Guermouche, J.-Y. L'Excellent, and S. Pralet, *Hybrid scheduling for the parallel solution of linear systems*, Parallel Computing, **32**(2006), 136–156.
- [Ba*19] S. Balay et al, *PETSc Users Manual*, ANL-95/11 - Revision 3.11, Argonne National Laboratory, 2019
- [Ba*97] S. Balay, W.D. Gropp, L. Curfman McInnes and B.F. Smith, *Efficient Management of Parallelism in Object Oriented Numerical Software Libraries*, Modern Software Tools in Scientific Computing, edited by E. Arge and A. M. Bruaset and H. P. Langtangen, 163–202, Birkhäuser Press, 1997
- [BGR82] C. Bardos, J.-C. Guillot and J. Ralston, *La relation de Poisson pour l'équation des ondes dans un ouvert non borné. Application à la théorie de la diffusion*, Comm. Partial Differential Equations **7**(1982), 905–958.
- [Ber*98] A. Bermúdez and L. Hervella-Nieto and A. Prieto and R. Rodríguez, *An exact bounded PML for the Helmholtz equation*, C. R. Acad. Sci. Paris, Ser.I **339**(2004).
- [BK62] M.Sh. Birman and M.G. Kreĭn, *On the theory of wave operators and scattering operators*, Dokl. Akad. Nauk. SSSR **144**(1962), 475–478.
- [Bu75] V. Buslaev, *Local spectral asymptotic behavior of the Green's function in exterior problems for the Schrödinger operator*, Collection of articles dedicated to the memory of Academician V. I. Smirnov. Vestnik Leningrad. Univ. No. 1 Mat. Meh. Astronom. Vyp. **1**(1975), 55–60.
- [Ch83] J. Cheeger, *Spectral geometry of singular Riemannian spaces*, J. Differential Geom., **18**(1983), 575–657.
- [Ch98] T. Christiansen, *Spectral asymptotics for compactly supported perturbations of the Laplacian on \mathbb{R}^n* , Comm. Partial Differential Equations, **23**(1998), 933–948.
- [ChDa22] T. Christiansen and K. Datchev, to appear.
- [DyGu13] S. Dyatlov and C. Guillarmou, *Scattering phase asymptotics with fractal remainders*, Comm. Math. Phys. **324**(2013), 425–444.
- [DyZw19a] S. Dyatlov and M. Zworski, *Mathematical theory of scattering resonances*, Graduate Studies in Mathematics **200**, AMS 2019, <http://math.mit.edu/~dyatlov/res/>
- [GLS21] J. Galkowski, D. Lafontaine and E. Spence, *Perfectly-matched-layer truncation is exponentially accurate at high frequency*, [arXiv:2105.07737](https://arxiv.org/abs/2105.07737).
- [JeKa78] A. Jensen and T. Kato, *Asymptotic behavior of the scattering phase for exterior domains*, Comm. Partial Differential Equations **3**(1978), 1165–1195.
- [HaZe99] A. Hassell and S. Zelditch, *Determinants of Laplacians in exterior domains*. Internat. Math. Res. Notices **18**, 971–1004 (1999).
- [He12] F. Hecht, *New development in FreeFem++*, Journal of numerical mathematics, **20**(2012), 251–266.
- [HöI] L. Hörmander, *The Analysis of Linear Partial Differential Operators I. Distribution Theory and Fourier Analysis*, Springer Verlag, 1983.
- [HöIII] L. Hörmander, *The Analysis of Linear Partial Differential Operators III. Pseudo-Differential Operators*, Springer Verlag, 1985.
- [Iv16] V. Ivrii, *100 years of Weyl law*, Bull. Math. Sci. (2016) <http://link.springer.com/journal/13373>
- [LSW21] D. Lafontaine, E. Spence and J. Wunsch, *For most frequencies, strong trapping has a weak effect in frequency-domain scattering*, Comm. Pure. Appl. Math., **74**(2021), 2025–2063.
- [Ka78] T. Kato, *Monotonicity theorems in scattering theory*, Hadronic J. **1** (1978), 134–154.
- [MaRa78-79] A. Majda and J. Ralston, *An analogue of Weyl's theorem for unbounded domains. I, II, III*, Duke Math. J. **45**(1978), 183–196, 513–536, **46**(1979), 725–731.

- [MaRo15] R. Mazzeo, and J. Rowlett, *A heat trace anomaly on polygons*, Mathematical Proceedings of the Cambridge Philosophical Society, **159**(1015),303–319.
- [McG13] I. McGillivray, *The spectral shift function for planar obstacle scattering at low energy*. Math. Nachr. **286**, 1208–1239 (2013).
- [Me88] R. Melrose, *Weyl asymptotics for the phase in obstacle scattering*, Comm. Partial Differential Equations **13**(1988), 1431–1439.
- [DLMF] *NIST Digital Library of Mathematical Functions*. <http://dlmf.nist.gov/>, Release 1.1.0 of 2020-12-15. F. W. J. Olver, A. B. Olde Daalhuis, D. W. Lozier, B. I. Schneider, R. F. Boisvert, C. W. Clark, B. R. Miller, B. V. Saunders, H. S. Cohl, and M. A. McClain, eds.
- [PePo82] V. Petkov and G. Popov, *Asymptotic behaviour of the scattering phase for nontrapping obstacles*, Ann. Inst. Fourier (Grenoble) **32**(1982), 111–149.
- [PeZw99] V. Petkov and M. Zworski, *Breit–Wigner approximation and distribution of resonances*, Comm. Math. Phys. **204**(1999), 329–351, Erratum, Comm. Math. Phys. **214**(2000), 733–735.
- [Ro94] D. Robert, *A trace formula for obstacles problems and applications*, Mathematical results in quantum mechanics (Blossin, 1993), 283–292, Oper. Theory Adv. Appl., 70, Birkhäuser, Basel, 1994.
- [Ra78] J. Ralston, *Addendum to: “The first variation of the scattering matrix”* (J. Differential Equations **21**(1976), no. 2, 378–394) by J. W. Helton and Ralston. J. Differential Equations **28**(1978), no. 1, 155–162.
- [SaVa97] Yu. Safarov and D. Vassiliev, *The asymptotic distribution of eigenvalues of partial differential operators*. Translations of Mathematical Monographs, **155**, AMS 1997
- [Sa20] J.J. Sakurai and J. Napolitano, *Modern Quantum Mechanics*, 3rd Edition, Cambridge University Press, 2020.
- [St99] P. Stefanov, *Quasimodes and resonances: sharp lower bounds*, Duke Math. J. **99**(1999), 75–92.
- [St01] P. Stefanov, *Resonance expansions and Rayleigh waves*, Math. Res. Lett., **8**(2001), 107–124.
- [StWa20] A. Strohmaier and A. Waters, *Geometric and obstacle scattering at low energy*, Communications in Partial Differential Equations **45**(2020), 1451–1511.
- [TZ98] S.H. Tang and M. Zworski, *From quasimodes to resonances*, Math. Res. Lett. **5**(1998), 261–272.
- [Va22] L. Vacossin, *Spectral gap for obstacle scattering in dimension 2*, [arXiv:2201.08259](https://arxiv.org/abs/2201.08259), to appear in Analysis & PDE.
- [Be1994] J.-P. Bérenger, *A perfectly matched layer for the absorption of electromagnetic waves*, Journal of Computational Physics, **114**(1994), no 2, 185–200.
- [CoMo98] F. Collino and P. Monk, *The Perfectly Matched Layer in Curvilinear Coordinates*, SIAM Journal on Scientific Computing, **19**(1998), no 6, 2061–2090.
- [DuWu15] Y. Du and H. Wu *Preasymptotic Error Analysis of Higher Order FEM and CIP-FEM for Helmholtz Equation with High Wave Number*, SIAM Journal on Numerical Analysis, **53**(2015), no 2, 782–804.
- [MGSS22] P. Marchand and J. Galkowski and A. Spence and E. A. Spence *Applying GMRES to the Helmholtz equation with strong trapping: how does the number of iterations depend on the frequency?*, Advances in Computational Mathematics, **48**(2022), no 4.
- [ErGu22] A. Ern and J.-L. Guermond, *Theory and Practice of Finite Elements*, Springer New York, **159**(2004).

18 JEFFREY GALKOWSKI, PIERRE MARCHAND, JIAN WANG, AND MACIEJ ZWORSKI

DEPARTMENT OF MATHEMATICS, UNIVERSITY COLLEGE LONDON, WC1H 0AY, UK

Email address: pierre.marchand@inria.fr

UNITÉ DE MATHÉMATIQUES APPLIQUÉES DE ENSTA PARIS, 91762 PALAISEAU CEDEX

Email address: wangjian@email.unc.edu

DEPARTMENT OF MATHEMATICS, UNIVERSITY OF NORTH CAROLINA, CHAPEL HILL, NC 27599

Email address: zworski@berkeley.edu

DEPARTMENT OF MATHEMATICS, UNIVERSITY OF CALIFORNIA, BERKELEY, CA 94720